C. R. Mecanique 341 (2013) 100–109

Contents lists available at SciVerse ScienceDirect

Comptes Rendus Mecanique

www.sciencedirect.com

Combustion, flow and spray dynamics for aerospace propulsion

Experimental investigation of cryogenic flame dynamics under transverse acoustic modulations

Yoann Méry [a,b], Layal Hakim [a,b,*], Philippe Scouflaire [a,b], Lucien Vingert [c], Sébastien Ducruix [a,b], Sébastien Candel [a,b]

[a] CNRS, UPR 288, laboratoire d'énergétique moléculaire et macroscopique, combustion (EM2C), grande voie des vignes, 92290 Châtenay-Malabry, France
[b] École centrale Paris, grande voie des vignes, 92290 Châtenay-Malabry, France
[c] ONERA, département d'énergétique fondamentale et appliquée (DEFA), BP 81000, 91120 Palaiseau, France

ARTICLE INFO

Article history:
Available online 9 January 2013

Keywords:
Combustion
Transverse acoustic modulations

ABSTRACT

The present investigation is focused on high-frequency combustion instabilities coupled by transverse acoustic modes. This phenomenon has been observed during the development of many liquid rocket engines and other high performance devices. Such instabilities induce an unsteady heat release which leads in many cases to a rapid intensification of heat fluxes to the thrust chamber walls, causing fatal damage and a spectacular destruction of the propulsion system. One central objective of this effort is to observe and understand the physical processes leading the coupling between acoustics and combustion, and resulting in the growth of such instabilities. Experiments carried out on the Mascotte testbed at ONERA serve to identify the main processes involved and bring forth mechanisms taking place when an engine becomes unstable. Hot fire experiments are carried out in a model scale combustor reproducing many of the conditions prevailing in unstable rocket engines. Subcritical and transcritical cryogenic jets are injected in a multiple injector combustion chamber (MIC). This system is fed with LOx and methane through five injection units. The flames formed in this configuration are modulated by an acoustic wave with an amplitude of several bars. This is obtained with a new Very Large Amplitude Modulator (VHAM) capable of generating acoustic mode amplitudes representative of those found in actual engine undergoing HF instabilities. It is shown first that the strength of the acoustic field and the frequency range of oscillation (1 kHz–3.5 kHz) are consistent with rocket instability observations. Conditions where a feedback of the flame on the acoustic field occurs are obtained. High speed diagnostics indicates that the velocity field dramatically enhances the atomization process. The liquid core length is strongly reduced. At moderate amplitudes, the liquid jets are flattened in the spanwise direction and heat release takes place in two sheets neighboring the dense core of oxygen. At higher amplitudes the core size is diminished and the flame pattern is considerably more compact. It is also shown that the flames are periodically displaced by the acoustic field and an alternate pattern of liquid oxygen appears in the chamber. An oscillation of the oxygen distribution in the transverse direction of the chamber is observed.

* Corresponding author at: CNRS, UPR 288, Laboratoire d'Énergétique Moléculaire et Macroscopique, Combustion (EM2C), Grande Voie des Vignes, 92290 Châtenay-Malabry, France.

E-mail addresses: yoann.mery@snecma.fr (Y. Méry), layal.hakim@ecp.fr (L. Hakim), philippe.scouflaire@ecp.fr (P. Scouflaire), lucien.vingert@onera.fr (L. Vingert), sebastien.ducruix@ecp.fr (S. Ducruix), sebastien.candel@ecp.fr (S. Candel).

1631-0721/$ – see front matter
http://dx.doi.org/10.1016/j.crme.2012.10.013

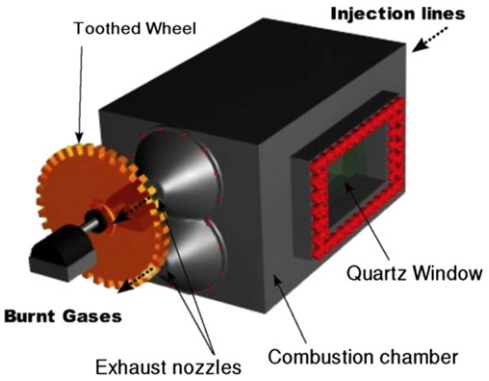

Fig. 1. MIC equipped with the VHAM.

1. Introduction

High-Frequency (HF) instabilities are observed in many high performance devices like liquid rocket engines. They involve a strong coupling between fluid dynamics, combustion and resonant modes of the chamber. Both longitudinal and transverse (radial and azimuthal) modes are involved in this process. Rocket engine hot fire tests indicate that transverse modes and in many cases rotating modes are the most destructive ones because they are less susceptible to damping by the nozzle and their amplitudes may reach very high levels. The acoustic mode enhances the combustion process, shortening the flame, augmenting the heat flux to the chamber walls and injection plane often leading to a rapid destruction of the system.

The experimental description of high-frequency instabilities is generally incomplete. Tests mainly provide pressure records obtained from a limited number of sensors. Most of the HF instability observations correspond to tests carried out during the development of new engines precluding data collection on the unstable combustion process. Systematic experiments were carried out during such developments and extensive efforts were necessary to deal with instabilities and modify the initial design by adding baffles, resonators or cavities to reduce the level of oscillation and check that the system could operate in a stable manner. Much of the available material obtained during the 1960s and early 1970s, an intense period of research on the subject, is gathered in a classical report by Harrje and Reardon [1]. The story of the costly trial and error process followed to suppress instabilities in the F1 engine is synthesized in a comprehensive article by Oefelein and Yang [2]. The combustion process was not visualized in the full scale tests for practical reason, and because the objective was not so much to gain a fundamental understanding but merely to find solutions to the problem. This did not allow detailed analysis of the driving mechanisms. The state of the art in the 1990s is summarized in an edited book by Yang and Anderson [3]. Since the development of new diagnostic tools, a limited number of experiments have been carried out on smaller scale engines to understand the driving processes and guide modeling efforts. More recent investigations on model scale facilities have allowed an optical access to the combustion process and simultaneous recordings of the pressure field on the combustor side walls (see for example Richecoeur et al. [4]). These new experiments are intended to study the link between the acoustic oscillations and the unsteady heat release. This is accomplished by examining the flame dynamics resulting from the acoustic perturbation with high speed cameras and time resolved optical and pressure sensors. Experiments of this type are now being carried out by different research teams and in particular by groups engaged in the French–German REST (Rocket Engine STability) program and in the American ALREST (Advanced Liquid Rocket Engine Stability Technology) framework.

Experiments reported in the present article were carried out on the cryogenic combustion test facility “Mascotte” of ONERA equipped with a multiple injector combustor (MIC). The MIC features five coaxial LOx/methane injectors and enables to observe flames under subcritical or transcritical conditions. The injection temperature is below the critical temperature of oxygen and the chamber mean pressure may take values in excess of 60 bar, well above the critical pressure of oxygen ($p_c(LOx) = 50.4$ bar). Previous work [4] has already provided information on the interaction of transverse acoustic modes with the multiple jet flame configuration established in the MIC. However, the oscillation level, reaching in one case about 8% of the chamber pressure, was still too low to represent the very high oscillation amplitudes prevailing in rocket engine thrust chambers undergoing high frequency instability conditions. It was then decided to abandon the initial set-up used in the MIC experiments and design a novel “very high amplitude modulator” (VHAM), a modulation system which could generate higher acoustic amplitudes under resonant conditions. This actuator comprises a rotating toothed wheel with a variable angular velocity. The principle of the VHAM is to modulate the total mass flow rate injected in the chamber using two exit nozzles, one located on the top of the chamber, another on the bottom (Fig. 1). These nozzles are alternately closed by the toothed wheel which creates an intense transverse excitation in the chamber. One important difference is that the rectangular geometry cannot sustain the rotating modes found in axisymmetric geometries of the type used in rocket thrust chambers.

The concept and some applications of the VHAM under cold flow conditions have already been described in [5]. It was for example possible to generate a powerful transverse acoustic field in a transparent pressurized cavity and characterize

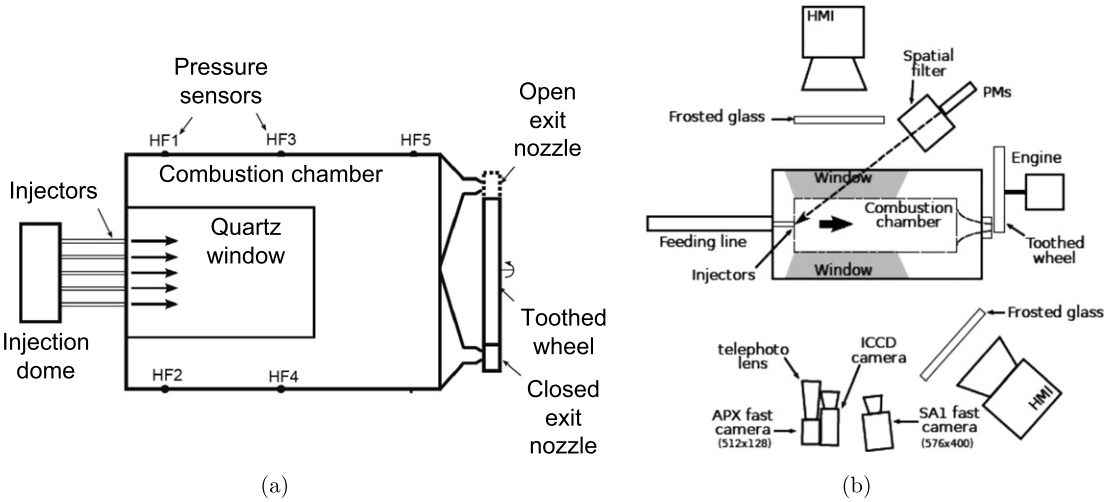

Fig. 2. (a) Combustion chamber equipped with the VHAM actuator and five pressure transducers. HF1, HF3 and HF5 (odd numbered sensors) are placed on the upper wall. HF2 and HF4 (even numbered sensors) are located on the lower wall. (b) Top view of the optical diagnostics arrangement. HMI designate continuous light spots. The photo-multiplier tubes PMT1 and PMT2 (designated as PMs on the drawing) are located on a vertical line and point towards the injection plane.

the acoustic velocities induced by the VHAM with PIV (particle imaging velocimetry). The VHAM is here used under hot fire conditions to excite transverse modes and analyze their impact on flame dynamics. The influence of several parameters is investigated, by varying the mean pressure in the chamber and the momentum flux ratio of the injected propellants. It is then possible to scan the different eigenmodes and observe the flame motion. The first objective is to link the flame dynamics to the acoustic modes. This is accomplished by examining pressure sensor signals, photo-multiplier signals and images recorded by two high speed cameras. These data are complemented by images of the mean flame shape under acoustic modulation as observed with an intensified CCD camera operating at a low frame rate.

2. Experimental setup

The study of high frequency combustion dynamics requires a combination of sensors and imaging methods discussed in the next subsection. These tools are exploited in an experimental procedure including linear frequency sweep experiments which are mainly used to identify the eigenmodes of the system and continuous wave modulation tests at the various resonant frequencies. This procedure is explained next.

2.1. Diagnostics

The MIC is equipped with five pressure sensors located on the top and bottom walls of the chamber (see Fig. 2 (a)) and operating in the dynamic mode to record the unsteady variations of pressure. The signals detected by the wall sensors can be used for modal identification. One additional pressure sensor, set in steady mode, provides the mean pressure in the chamber. The mean temperature in the chamber is measured by a type K thermocouple inserted in the bottom wall of the chamber. All the dynamic pressure sensors are sampled at a rate of 40 kHz. The mean pressure sensor and the thermocouple are recorded at 10 Hz.

Fig. 2 (b) shows a top view of the optical diagnostics arrangement. This includes three cameras and two photo-multipliers. The Photron Fastcam SA1 camera operates at a frame rate of 24 kHz. This camera provides a view of the complete combustion chamber with an image size of 576×400 pixels and a resolution of 263 µm/pixel (38 pixel/cm). It is equipped with a Nikkor lens of 105 mm and a CH^* filter. The other high speed camera, the Photron Fastcam APX, also operates at 24 kHz and is synchronized with the Fastcam SA1. It focuses on the central jet. The image size is 512×128 pixels and the resolution is 204 µm/pixel (49 pixel/cm). This camera is equipped with a Nikkor telephoto lens (80–200 mm, set at 200 mm), and operates in a backlighting mode to locate the position and dynamics of the dense oxygen jet, droplets or packets. Light is emitted by the HMI spot located in front of the cameras (Fig. 2 (b)). It should be noted that the SA1 camera detects a part of the white light emitted by the spot, even when a filter is used to isolate the light emitted by CH^* radicals. To avoid an important bias, a careful setting of the imaging diagnostic is needed and requires a trade-off involving the intensity of the HMI spot, exposure time and aperture of the cameras. Since this trade-off strongly depends on the light emitted by the flame, which is difficult to predict, it is necessary to adjust the light level by a trial and error process, which depends on the operating point conditions. An intensified camera (ICCD), providing a high dynamic range (16 bit), is also used. The field of view encompasses major parts of the chamber. It is equipped with a Nikkor UV lens (105 mm focal) and an OH^* filter (88SA centered on 313 nm). In the present case, the critical benefit of OH^* spontaneous emission compared

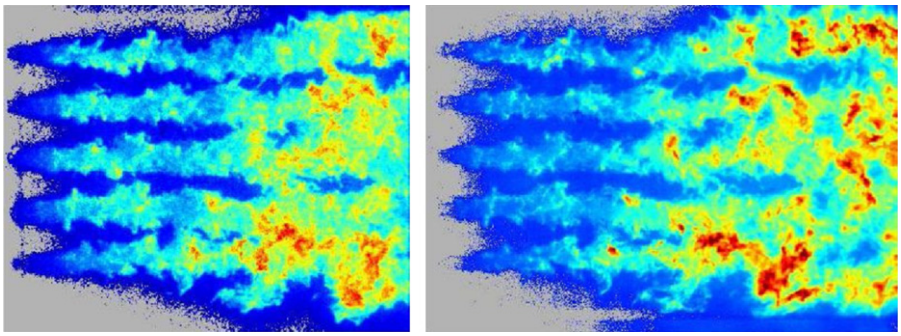

(a) OH* (b) CH*

Fig. 3. (a) ICCD and (b) SA1 images taken at the same instant. The flame structure is similar, which establishes consistency between the two diagnostics (at a mean chamber pressure of 59 bar and in the absence of external modulation (OWM)).

Table 1
Operating points studied during the hot fire tests. Injection temperature for methane and liquid oxygen are kept constant at $T_{CH_4} = 280$ K and $T_{LOx} = 80$ K respectively.

Points	p_{ch} (MPa)	E	J
PF1	1.0	1.3	5
PF2	2.6	1.33	2
PF3	2.6	1.33	6
PF4	5.9	1.13	3.8
PF5	5.9	1.13	11.3

with CH* one is that its wavelength is located in the near UV of the light spectrum. The white light created by the HMI has a negligible contribution in the UV range and no interferences are observed between the two diagnostics. The ICCD camera records images at a low rate (approximately 15 Hz) and thus cannot be used to study the dynamics of the process. Because this camera operates continuously during the test case it provides interesting information on the mean shape of the flame during the entire test.

At this point it is interesting to see if the different optical diagnostics yield consistent data. This is done by comparing the high dynamic range OH* images obtained with the ICCD camera and the high speed CH* data obtained with the SA1 camera (Fig. 3). Each image is normalized by its own maximum value. One finds that images obtained at the same instant are quite similar, with only minor differences and that the OH* and the CH* emission distributions have similar structures.

In addition to high speed images two photo-multiplier tubes (PMT) equipped with OH* filters record time resolved signals corresponding to free radicals emitted from the flames: PMT1 detects OH* radiation from the upper part of the chamber while PMT2 records OH* radiation from the lower part. This arrangement is used to obtain the time evolution of the heat release rate in the transverse direction of the chamber, which plays a key role in the understanding of HF coupling between combustion and transverse modulations. A spatial filter, reducing the solid angle, is placed in front of the PMT sensors so that the upper PMT does not detect light emitted from the lower part of the chamber, and vice versa. In Fig. 2 (b), the photo-multiplier tubes are oriented to record light originating from the injector near field. The PMT signals are recorded at a rate of 40 kHz, during the whole hot fire tests.

2.2. Experimental procedure

Injection conditions have been chosen to study the influence of flow parameters such as mean pressure, momentum flux ratio, mixture ratio, etc. The flow parameters corresponding to the operating points are gathered in Table 1, where

$$J = \frac{\rho_{CH_4} v_{CH_4}^2}{\rho_{LOx} v_{LOx}^2} \quad \text{and} \quad E = \frac{\dot{m}_{LOx}}{\dot{m}_{CH_4}}$$

Three mean pressures are investigated. PF1 is defined to allow comparison with results obtained during previous hot fire tests carried out on the Mascotte facility. The difference between PF2 and PF3 and between PF4 and PF5 is the momentum flux ratio J. For all tests, the mixture ratio E is kept nearly constant. Injection temperature for methane and liquid oxygen are also kept constant at $T_{CH_4} = 280$ K and $T_{LOx} = 80$ K respectively.

The experimental procedure is specifically designed to study the coupling of transverse acoustic modes and multiple cryogenic jet flames. To obtain the largest amplitudes, it is important to identify the resonant modes of the system. The method consists in imposing a constant acceleration to the wheel to obtain a linear frequency modulation (LFM).

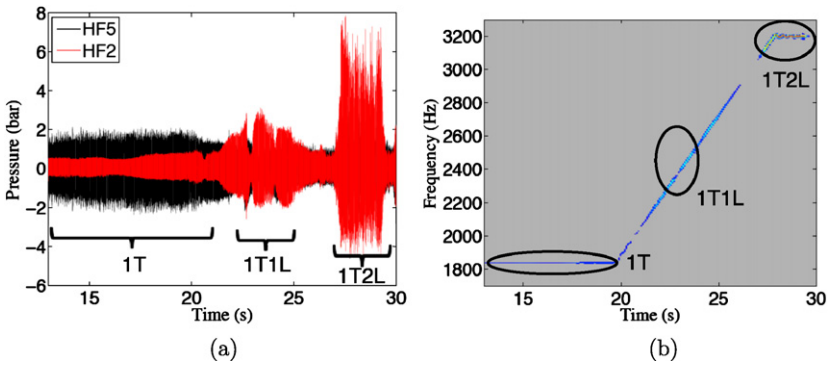

Fig. 4. PF2 during a linear frequency modulation test. (a) Pressure sensor response. (b) Corresponding evolution of HF2 power spectral density in the time-frequency domain.

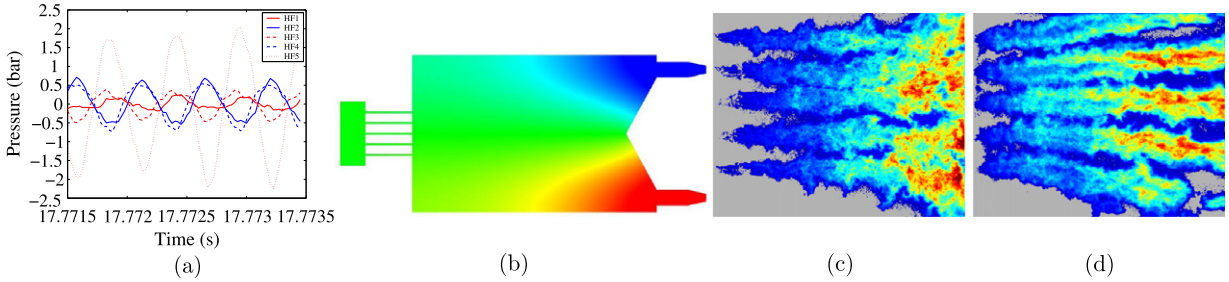

Fig. 5. PF2. (a) Response of the pressure transducers during a 1T CWM. (b) Normalized spatial pressure distribution calculated for the 1T eigenfrequency (red: 1; blue: −1). (c) Instantaneous OH* emission of the flames without any modulation and (d) during 1T continuous wave modulation.

The frequency is swept linearly in a range which contains the expected eigenfrequencies. Signals recorded by the pressure transducers are then processed to determine the short time spectral content and identify the eigenmodes, which correspond to the maximum response. This is illustrated in Fig. 4 where the wheel is accelerated from 1800 Hz to 3200 Hz. In this range, three pressure peaks emerge from the background noise. They correspond to the first three transverse eigenmodes. Values of the system eigenfrequencies identified in the first step are then used in continuous wave modulation (CWM) tests in order to study combustion dynamics under resonant conditions. It is also important to use baseline operating conditions to examine combustion in the absence of modulation. In the present configuration this is not easy to obtain because the VHAM has to be removed and the nozzle throat diameter has to be modified to keep the same mass flow rate. An alternative method consists in using as a reference the system operating with a wheel rotating at low frequency under off-resonant conditions. This methodology is applied to each operating point under investigation (PF1 to PF5). During the hot fire tests, the modes observed for the different operating points were quite similar in frequency as in structure, whatever the injection conditions. This was confirmed a posteriori by comparing information obtained for the different operating points and numerical estimates and precisely identifying the various modes. Numerical estimates of the shapes and frequencies of successive eigenmodes were obtained using AVSP [6,7], a Helmholtz solver developed by CERFACS. In these calculations, temperature is uniform in the domain and a vanishing velocity is prescribed on the solid boundary conditions while the nozzle exhausts are represented by an acoustic admittance [8].

3. Flame response to strong acoustic modulations

In this section, we highlight some of the common elements observed under resonant conditions. For this we specifically consider the PF2 test case under 1T and 1T2L modulations. It is found that the 1T2L mode induces the strongest combustion response and the highest level of pressure oscillation but it is also interesting to examine what happens at lower modulation amplitudes. Two main effects can be brought out: (1) the acoustic modulation modifies the mean flame structure and (2) the flames are set into a transverse motion, following the acoustic field and subsequently generating heat release rate fluctuations.

3.1. Modification in the flame structure

For all operating points, the flame structure is modified by the acoustic modulation. When the amplitude of modulation is moderate, the expansion angle is enhanced and the reacting zone is flattened. This is shown in Fig. 5 for operating point PF2 during a 1T continuous wave modulation at 1.8 kHz. The pressure signals in Fig. 5 (a) correspond well to the first

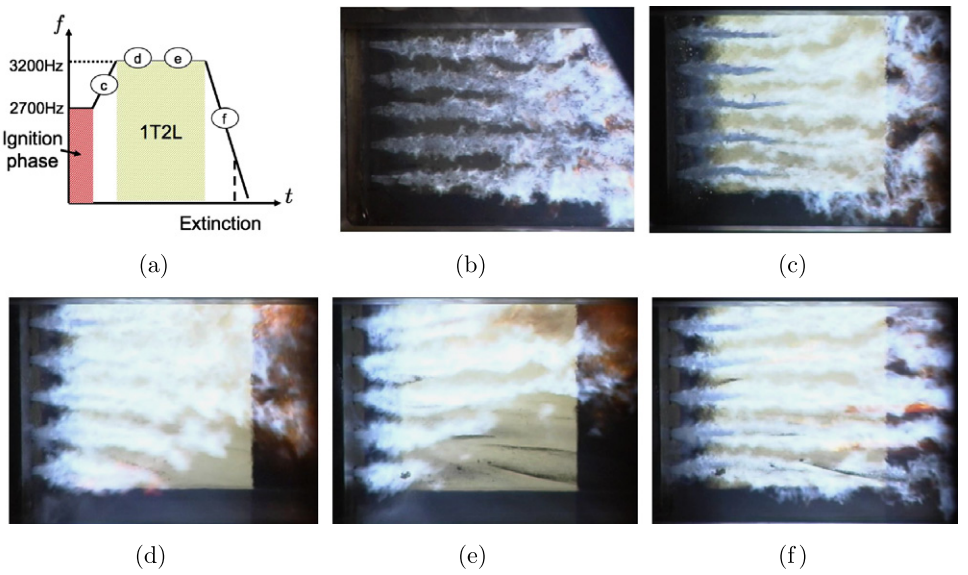

Fig. 6. PF2. Flames recorded by a DV control camera. (a) Schematic description of the hot fire test showing the different instants at which each image is taken: (b) without any modulation; (c) during the ramp to the 1T2L frequency; (d) at the beginning of the 1T2L mode; (e) at the end of the 1T2L mode; (f) during the ramp to extinction.

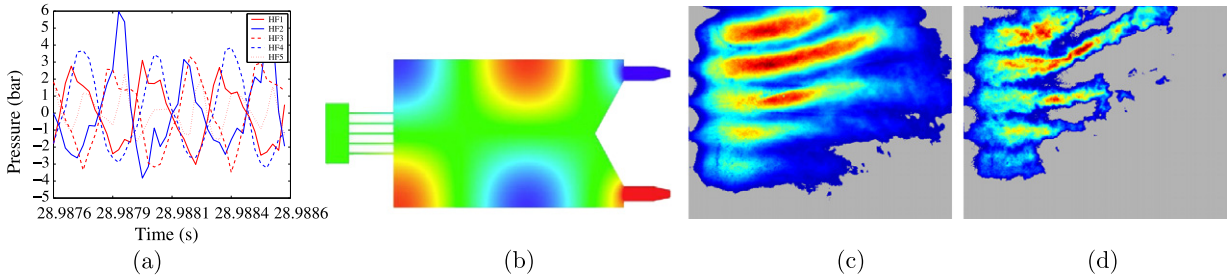

Fig. 7. PF2. (a) Response of the HF pressure transducers during a 1T2L CWM. (b) Normalized spatial pressure distribution calculated for the 1T2L eigenfrequency (red: 1; blue: −1). (c) Instantaneous OH* emission. (d) Average OH* emission. Flames are short. Those in the upper part of the chamber are longer than those established in the lower part.

transverse mode structure. HF1, HF3 and HF5 are in phase and in opposition with HF2 and HF4. The pressure oscillation amplitude near the injection plane (HF1 and HF2) is about 1 bar peak-to-peak and it is lower than in the aftplane (HF5) as expected from the calculation of this 1T mode (Fig. 5 (b)). Without any modulation (Fig. 5 (c)), the dense liquid oxygen core is not visible and one can only see the flames. In the modulated case (Fig. 5 (d)), one can clearly distinguish the five dense cores, corresponding to the five coaxial injectors, each one bounded by two thin flame layers. It is likely that this modification in the heat release rate pattern is linked to a modification of the liquid jet geometry which, when submitted to strong transverse acoustic velocity, forms a sheet in the spanwise direction accelerating its break-up and enhancing secondary atomization. This phenomenon was already observed in cold flow experiments of a jet under transverse acoustic modulations (see [9] and references therein). The spray characteristics are modified and the rate of vaporization is increased generating upper and lower layers of gaseous oxygen feeding the neighboring flame sheets.

While double layer flames prevail under moderate oscillation amplitudes, a new pattern appears when the pressure oscillation reaches a higher level. The flames become notably shorter and the symmetry is broken. This is what happens under PF2 conditions with an enhanced level of modulation at a frequency of 3.2 kHz corresponding to the 1T2L mode. At this frequency, the peak-to-peak pressure recorded by the HF transducers at the end of the test is about 12 bar, which is nearly one half of the mean pressure in the chamber (26 bar). Fig. 6 shows a direct visualization of the flames during a typical hot fire test case. These images recorded by a DV control camera illustrate how the flame structure is modified depending on the acoustic modulation. In this test the rate of rotation of the toothed wheel is varied. The frequency is initially set at an off-resonance value of 2.7 kHz. The frequency is then swept linearly reaching the 1T2L value and it is then kept constant for a long period of time. The wheel is then decelerated at the end of the test.

The flames become much shorter when the resonant conditions are reached. This can be seen by comparing off-resonant conditions appearing in Fig. 6 (b) with fully resonant conditions prevailing in Fig. 6 (e). This is also visible by comparing Figs. 7 (a) and 5 (c). One also notices that under resonant conditions the flames are directed upwards. Under high amplitudes

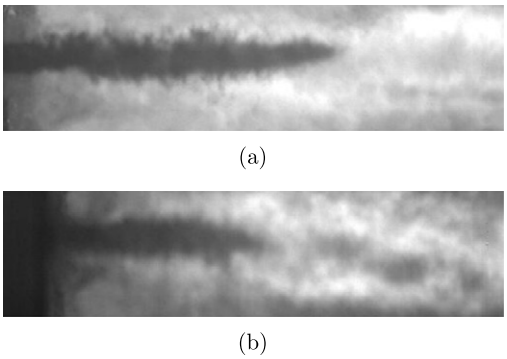

Fig. 8. Instantaneous backlighting images of the dense jet. (a) 1T CWM. (b) 1T2L CWM.

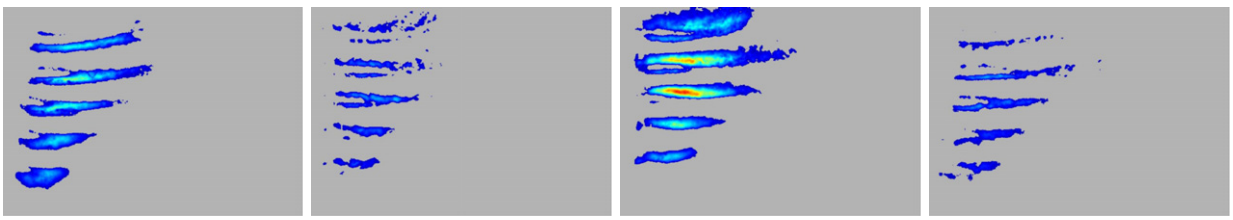

Fig. 9. PF2 during 1T2L CWM. Phase-averaged images of CH* (a) at $\phi = \pi/2$; (b) at $\phi = \pi$; (c) at $\phi = 3\pi/2$; (d) $\phi = 2\pi$. Phase is related to pressure distribution. $\phi = 0$ corresponds to a uniform pressure distribution in the chamber. $\phi = \pi/2$ corresponds to HF1 minimum and HF2 maximum.

of oscillation the liquid jet break-up is accelerated to an even greater level and the intensity of combustion is enhanced. This is visible in Fig. 8 where the liquid dense core is seen to be much shorter as the modulation level is augmented giving rise to compact flames. As most of the heat release takes place near the injection plane, the heat flux is intensified and this may eventually damage the injectors.

3.2. Acoustic coupling and modification in the flame dynamics

In addition to the changes observed in the mean field, an examination of the high speed films indicates that the flame dynamics is also strongly affected by the acoustic perturbations. High speed images reveal a synchronized oscillation of the five flames in the transverse direction at the frequency of modulation. This motion can be extracted by eliminating disturbances due to turbulence. To do so, phase-averaged images of CH* emission are calculated. The mean value is first subtracted, giving access to a qualitative representation of the unsteady heat release rate $\dot{q}'(\mathbf{x}, t) = \dot{q}(\mathbf{x}, t) - \bar{\dot{q}}(\mathbf{x})$. The periodic fluctuation is then obtained by calculating the phase average $\dot{q}'(\mathbf{x}, \phi)$ of $\dot{q}'(\mathbf{x}, t)$. One finds that the pattern of light emission is periodically displaced in the transverse direction and that this displacement is synchronized by the pressure field. This can be observed in Fig. 9 under PF2 conditions during a 1T2L mode showing phase-averaged images of CH* at four different phases ϕ in one cycle. When $\phi = \pi/2$, $\dot{q}'$ globally recorded by PMT1 in the upper part of the chamber is smaller than when $\phi = 3\pi/2$. The opposite is true for PMT2.

The intensity of light emission increases indicating that the amplitude of heat release fluctuations also increases augmenting the volumetric rate of heat release (see Fig. 10 (a)). This mechanism effectively induces the growth of pressure oscillations as illustrated in Fig. 10 (b). For this to be so, heat release and pressure fluctuations must be in phase as can be deduced from a balance of acoustic energy (see for example Poinsot and Veynante [10] for underlying assumptions):

$$\frac{\partial E}{\partial t} + \nabla \cdot \mathbf{F} = S - D \quad \text{with } E = \frac{1}{2}\bar{\rho}\mathbf{u}'^{\mathbf{2}} + \frac{1}{2}\frac{p'^2}{\bar{\rho}c^2},\ \mathbf{F} = p'\mathbf{u}' \text{ and } S = \frac{\gamma - 1}{\gamma \bar{p}} p'\dot{q}' \tag{1}$$

In Eq. (1), E, $\mathbf{F}$, S and D are, respectively, the acoustic energy density, the acoustic energy flux, the acoustic energy source and damping rate. $\mathbf{u}'$ and p' are the acoustic velocity and pressure. $\bar{\rho}$ is the mean density, γ the isentropic expansion factor and c the speed of sound. This instantaneous balance equation may be integrated over a period T of oscillation. The driving term S then becomes

$$\mathcal{S} = \frac{\gamma - 1}{\gamma \bar{p}} \int_T p'\dot{q}' \, \mathrm{d}t$$

When $\mathcal{S}$ is positive and exceeds the period average of the damping rate, the acoustic energy is augmented, a result which can be linked to the Rayleigh criterion. Equivalently, when the unsteady heat release rate is in phase with the

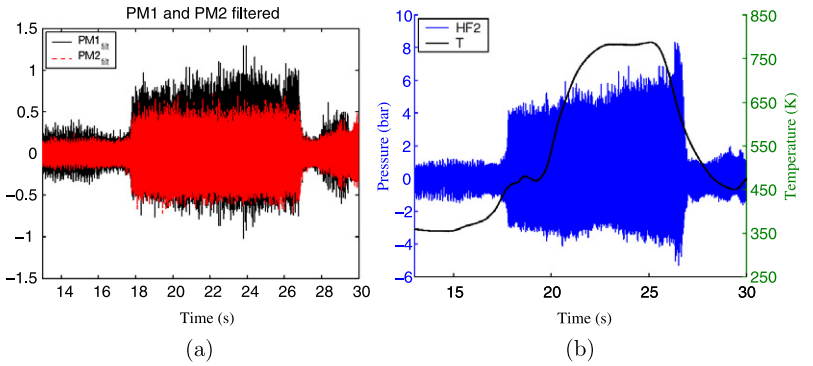

Fig. 10. PF2 during 1T2L CWM. (a) Filtered photomultipliers response. (b) HF2 response plotted together with the temperature recorded at the bottom wall of the chamber.

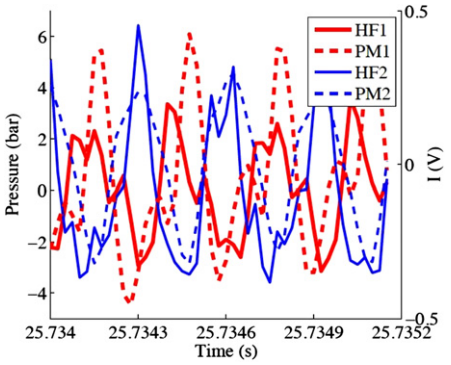

Fig. 11. PF2 during 1T2L CWM. Near injection pressure sensors HF1 and HF2 plotted with PMT signals during a few cycles of oscillation.

pressure oscillation, as shown in Fig. 11, $\mathcal{S}$ becomes positive and acts as a driving term, leading to an increase in the acoustic oscillation amplitude, confirming what is observed in Fig. 10 (b).

The pressure fluctuation amplitude increases during the test case, indicating a positive growth rate. Still, this growth rate is not high enough to compensate for the system damping and oscillations abruptly decrease in amplitude as soon as the modulation frequency is changed ($t = 26.7$ s in Figs. 10 (a) and 10 (b)). This also clearly shows the interest of the VHAM actuation, which is crucial to obtain a high amplitude coupling between flames and acoustics. One finally notes in Fig. 10 (b) that the temperature recorded at the bottom wall of the chamber rapidly increases, illustrating the well-known heat flux enhancement usually associated with combustion instabilities.

The streak film, displayed in Fig. 12, helps in investigating the mechanism leading to the asymmetry observed in the previous section. The method, used for example by Tischler and Male [11], consists in recording light emitted in a thin window defined as a rectangular slice in the transverse direction. The recording is formed at high frequency providing a space–time film of the light intensity in the window. Fig. 12 (b) shows that the flame near the lower part of the chamber oscillates with a higher amplitude than that established in the upper part of the chamber. The atomization process is differentially enhanced as can be seen in the flame length reduction which is more pronounced in the lower part of the chamber.

3.3. Origin of the unsteady heat release

Experimental results presented so far show that the unsteady heat release rate can be due to the flame motion induced by the acoustic field. However, the unsteady heat release may be linked to the pressure or the velocity field, and it is hard to discriminate between these two possibilities since acoustic velocity and pressure are related by the linearized momentum balance:

$$\rho_0 \frac{\partial \mathbf{v}}{\partial t} = -\nabla p$$

One may consider two possible coupling processes when an acoustic wave is assumed to be present in the combustion chamber to explain the previous observations:

– Transverse velocity enhances the liquid jet break-up, primary and secondary atomization associated with inertial stresses, augmenting the rate of vaporization of oxidizer and subsequently the rate of heat release.

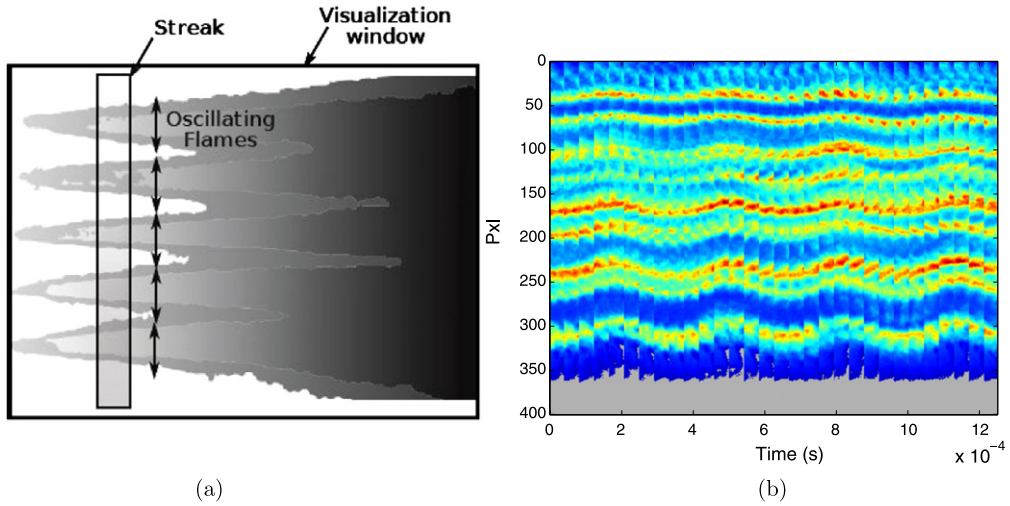

Fig. 12. PF2 during 1T2L CWM. (a) Schematic representation of the visualization window used to create the streak film. The motion of the flames is illustrated by setting side by side the same streak recorded at successive instants by the SA1 high speed camera equipped with CH^* filter. (b) Streak film deduced at 24 kHz.

– The acoustic pressure modifies the heating and vaporization of droplets, changing the mass rate of oxidizer generated per unit volume and therefore the rate of heat release.

Two reduced order models are derived from these observations [12], which are based on a methodology introduced by Zinn and Lores and applied in various studies by Culick and coworkers [13–15].

The first one (Flame Acoustic Motion Equation, FAME) is directly related to the experimental observations. It considers each flame as a thin line put into motion by the transverse acoustic velocity. The flame transverse position in time is then estimated as a function of the transverse acoustic velocity. As the unsteady heat release rate depends on this position, it can in turn directly be related to the transverse acoustic velocity, closing the source term in the acoustic balance equation.

The second model is more sophisticated and takes into account the liquid oxygen dynamics (Spray Dynamics Modeling, SDM). The shape of the flames is the result of complex atomization, vaporization and mixing processes. The inclusion of the liquid phase raises two challenges. First, liquid droplets show an inertia, which depends on their mass and bigger droplets do not follow the acoustic velocity. This introduces a delay associated to momentum relaxation. Secondly, droplets have a spatial density distribution, which strongly influences the local heat release rate. Using an eulerian framework and describing the liquid and gas phases through the balance equations for momentum and mass, one can link the fluctuations in liquid oxygen partial density to a delayed value of the local pressure disturbance. Then, making the assumptions that the atomization process results in a monodisperse spray and that combustion occurs instantaneously after vaporization, one can write the unsteady heat release rate as a function of this partial density and then as a function of the local pressure fluctuations, finally leading to the closure of the Rayleigh source term. Both models have been implemented recently in STAHF, a low order tool dedicated to combustion stability analysis [12], and tests are under way.

4. Conclusions

This article reports hot fire experiments carried out on a multiple injector combustor fed with liquid oxygen and gaseous methane. This system is modulated by a rotating toothed wheel periodically and alternately blocking one of the two nozzles exhausting the flow from the combustor. This new modulation method designated as VHAM induces powerful acoustic perturbations in the set-up with a level typically reaching 20% of the mean chamber pressure. Because the two nozzles are shut alternatively, transverse modes are promoted. The levels of oscillation and transverse character of the motion induced in the model setup are representative of the type of perturbations found when a high frequency instability arises in a liquid rocket engine. Backlighting images indicate that the acoustic modulation changes the atomization process. Under moderate levels of oscillations the liquid core is flattened and secondary atomization is enhanced, augmenting the vaporization rate. The level of available gaseous oxygen is enhanced in the neighborhood of the liquid sheet giving rise to two flame layers on the upper and lower side of the liquid sheet. When the level of oscillation reaches larger values, the liquid jet break-up is accelerated giving rise to shorter liquid cores and enhanced atomization and vaporization. This in turn greatly reduces the flame length augmenting the rate of heat release per unit volume. The combustion intensity is enhanced and this induces a rapid increase in the lateral wall temperature. The smaller droplets produced under strong transverse modulation closely follow the transverse acoustic velocity field and their vaporization and subsequent heat release is synchronized with the pressure field. It is found that the heat release regions oscillate in the transverse direction. Their displacement follows the

velocity field, a situation which gives rise to heat release rate fluctuations. Experiments reported in this article provide information on the unsteady combustion process coupled to transverse acoustic modes. It is shown that these data can be used to derive the physical mechanisms involved in this process. Satisfactory agreement could be obtained between experimental data and preliminary results, validating the methodology.

Acknowledgements

This work is supported by SAFRAN Snecma Space Engines Division, the prime contractor of the Ariane launcher cryogenic propulsion system, CNES and CNRS in the framework of the French–German program on Rocket Engines STability (REST).

References

[1] D.T. Harrje, F.H. Reardon, Liquid propellant rocket combustion instability, Technical Report SP-194, NASA, 1972.
[2] J.C. Oefelein, V. Yang, Comprehensive review of liquid-propellant combustion instabilities in F-l engines, Journal of Propulsion and Power 9 (5) (September–October 1993) 657–677.
[3] V. Yang, W. Anderson, Liquid Rocket Engine Combustion Instability, vol. 169, AIAA, 1995.
[4] F. Richecoeur, P. Scouflaire, S. Ducruix, S. Candel, High-frequency transverse acoustic coupling in a multiple-injector cryogenic combustor, Journal of Propulsion and Power 22 (4) (2006) 790–799.
[5] Y. Mery, S. Ducruix, P. Scouflaire, S. Candel, Injection coupling with high amplitude transverse modes: Experimentation and simulation, C. R. Mécanique 337 (2009) 426–437.
[6] C. Martin, L. Benoit, F. Nicoud, T. Poinsot, Analysis of acoustic energy and modes in a turbulent swirled combustor, in: Proc. of the Summer Program Stanford, Center of Turbulence Research, NASA Ames/Stanford Univ., 2004, pp. 367–375.
[7] F. Nicoud, L. Benoit, C. Sensiau, T. Poinsot, Acoustic modes in combustors with complex impedances and multidimensional active flames, AIAA Journal 45 (2) (2007) 426–441.
[8] F.E. Marble, S.M. Candel, Acoustic disturbance from gas nonuniformities convected through a nozzle, Journal of Sound and Vibration 55 (2) (1977) 225–243.
[9] F. Baillot, J.-B. Blaisot, G. Boisdron, C. Dumouchel, Behaviour of an air-assisted jet submitted to a transverse high-frequency acoustic field, Journal of Fluid Mechanics 640 (2009) 305–342.
[10] T. Poinsot, D. Veynante, Theoretical and Numerical Combustion, third ed., https://www.cerfacs.fr/elearning, 2011.
[11] A.O. Tischler, T. Male, Oscillatory combustion in rocket-propulsion engines, in: Gas Dynamics Symposium, 1956, pp. 71–81.
[12] Y. Méry, Mécanismes d'instabilités de combustion haute-fréquence et application aux moteurs-fusées, PhD thesis, Ecole Centrale, Paris, 2010.
[13] F.E.C. Culick, Nonlinear behavior of acoustic-waves in combustion chambers. 1, Acta Astronautica 3 (9–10) (1976) 715–734.
[14] F.E.C. Culick, Combustion instabilities in liquid-fueled propulsion system – an overview, in: AGARD Conf. Proceedings, Number 450, 1988.
[15] F.E.C. Culick, V. Yang, Overview of combustion instabilities in liquid-propellant rocket engines, in: Liquid Rocket Engine Combustion Instability, vol. 169, AIAA, Inc., Washington, DC, 1995, pp. 3–37.